IAES International Journal of Artificial Intelligence (IJ-AI)
Vol. 15, No. 2, April 2026, pp. 1999~2008
ISSN: 2252-8938, DOI: 10.11591/ijai.v15.i2.pp1999-2008

Improvised mask faster recurrent convolutional neural network for breast cancer classification using histopathology images

Pattan M. D. Ali Khan, Xavier Arputha Rathina
Department of Computer Science and Engineering, B. S. Abdur Rahman Crescent Institute of Science and Technology, Chennai, India

Article Info

Article history:

Received Jan 25, 2024
Revised Jul 27, 2025
Accepted Sep 8, 2025

Keywords:

Breast lesions
Classification
Deep learning
Histopathology images
Improved faster recurrent convolutional neural network

ABSTRACT

Despite the prevalence of this disease, the existing method for obtaining an exact breast cancer diagnosis would need a lot of time and labor. It needs a qualified pathologist to manually process and review histopathological images to distinguish the characteristics that characterize different cancer severity levels. Building a model for automatically detecting, segmenting, and classifying breast lesions using histopathological images seems to be the goal of this work. Various deep learning methods have been used in computational pathology for the diagnosis of cancer. Improved faster recurrent convolutional neural network (IMFRCNN) is a supervised learning system with proposed for recognizing small items like mitotic and non-mitotic nuclei. To protect small items from vanishing in the deep layers, this system uses expanded layers in the spine. To close image and the things gap size includes, this approach uses expanded layers. The region proposal network has been created for precise tiny object identification. Researchers examined time for training and testing time for various techniques for identifying objects. The total accuracy of benign/malignant categorization in proposed system reaches 96.5%. The proposed technique offers a thorough and non-invasive method for identifying and categorizes an area of abnormal breast tissue.

Corresponding Author:

Pattan M. D. Ali Khan
Department of Computer Science and Engineering
B. S. Abdur Rahman Crescent Institute of Science and Technology
Chennai, India
Email: alik_12@rediffmail.com

1. INTRODUCTION

Modern digital copies of glass slides were typically table-top equipment that scanned glass slides and provided whole-slide images quickly and affordably, frequently automating intermediary stages like tissue segmentation and focus plane choice [1]. The creation of a high-resolution digital photomicrograph for an entire histological or cytology slide was referred to as whole-slide photography [2]. Although tumors remain the most common type of cancer in women, a sizable portion of the samples examined in pathology labs come from individuals with the condition [3]. Hematoxylin eosin stains have endured as the go-to stain for histological examination of individual cells. The fine tissue and cell features can be highlighted by this straightforward dye mixture [4].

Similar to this, our method has made suitable therapy recommendations according to the lessons learned. Breast cancer refers to a disease of the brain cell that causes the cell to deteriorate while becoming inactive [5]. This would contribute to dementia. Deterioration of mental, behavioral, and effective communication was dementia symptoms that impair people's capacity for autonomous action. Cognitive problems make up one of the Alzheimer's disease's signs. The client might forget current occurrences in the

initial stages. As the illness worsens, someone would gradually lose details [6]. Sentiment analysis, electromyography signals diagnosis, and cardiovascular illness categorizations from an electrocardiogram (EKG) signal were some well-known machine learning applications in the biomedical field [7]. Using a microscope, histopathological images were acquired, and specimens of the breast tissue from the afflicted areas were collected. Hematoxylin and eosin have been utilized to stain the tissues to identify tumors [8]. Eosin colors the remainder of the cells pink, while hematoxylin gives the nucleus a dark purple color. By including a strong average percentage accuracy and recollection, tiny items could be detected and classified using the region-based convolutional neural network (RCNN). Tiny items disappearing in images would be a prevalent problem with deep learning models because small things have a high proportion variation between the image and the object. By nearly maintaining the geometry of the nucleus, the RCNN minimizes the loss of nuclei. This technique reduced the frequency of false negatives and false positives while aiding in the recovery of nucleus characteristics from the basal layer.

Imaging diagnostics include breast magnet resonance imaging (MRI), mammography, and breast ultra-sonography has become the preferred method of breast screening. Various imaging modalities were linked to various indications [9], [10]. Soft tissue lesions can easily be detected with MRI for screening the breast cancer. However, it's expensive, has a propensity for false positives, and takes a while to scan. As a result, breast MRI was primarily advised for women have a high risk of developing breast cancer [11]. Mammography has limits for those with dense breast tissue because of its great sensitivity to the identification of abnormal cells. The transducer transforms electrical signals into ultrasonic waves for breast imaging [12]. The reflected sound waves could be processed by a computer to produce an image based on the varying ultrasonic wave amplitudes and echoes times [13]. Ultra sonography has the benefit of real-time examination and no ionizing radiation [14]. Ultrasound can be utilized in medicine for echo-guided biopsy investigations. Nowadays, the most popular testing methods are mammography and breast ultra-sonography [15]. Also, it takes a lot of time and high level of expertise to differentiate between different subtypes of breast cancer using digital pictures created from biopsy samples that have been collected.

The staining procedure, lab procedures, and scanner brightness all produce significant color differences when creating histopathology images, making it difficult to effectively train a multi-class convolutional neural network (CNN) model, particularly in light of borderline instances [16]. Since digital images may well have clutter and insufficient brightness, image augmentation and preprocessing were crucial phases [17]. The effectiveness of extracting features and also the outcomes of image recognition could both be dramatically improved by picture preprocessing. The mathematical standardization of information gathering, a frequent step in many feature descriptor approaches, was akin to pretreatment [18]. To solve issues caused by color discrepancies, preprocessing must follow grayscale principles. Image enhancement aims to make photographs easier for viewers to understand or interpret or to give "better" input to other automated [19]. There have been two categories of image-enhancing techniques: frequency domain and spatial domain. The previous works with individual pixels directly, whereas the latter uses the image's Fourier transform [20], [21]. Typically speaking, an active contour system or a snake model based on curve assessment approaches would be employed. Moreover, a significant drawback of active contours was their failure to deal with shadowing or determine the boundaries of items that overlap them [22]–[25].

Size and shape were concepts included as part of the morph metric assessment. Analysis of an organism's fossil evidence seems to be a common procedure [26]. The effects of mutations on design, development, and modifications that take place, the shape's correlation with environmental parameters, and methods for assessing quantitative features of a certain shape [27]. For the cell and also the nucleus, the following morph metric features—increased mean values—were statistically significant: area, convex area, and outline [28]. Identification of items or regions of interest in an image using textural clues. By assessing feature points at every place in the image and deriving a collection of statistics from the distributions of the feature points, statistical techniques may be used in texture analysis to investigate the geographical extent of gray levels [29]. Discrete wavelet transforms, which typically classify images of malignant cells, are based on textural cues. The local binary pattern component, a potent technique utilized in computer vision and applications involving pattern recognition, has been presented here and employed for surface recognition and categorization [30]. Co-occurrence at the gray level, the characteristics of the matrix wavelet and the law's texture were retrieved. Here, the significance of the work is mentioned.

- By addressing the inter-class resemblance of tiny items while maintaining unique forms, the improved faster recurrent convolutional neural network (IMFRCNN) would be a useful concept for enhanced feature extraction.
- A critical challenge would be to count the dilated layers and utilize the dilating rate in each one.
- 3 dilated layers with a dilatation rate of 2 were employed in the proposed model to handle this crucial work without changing the morphology of mitotic nuclei.

– By making tiny objects larger, the proposed model corrects the mismatch between the image and object-covered areas in deep layers. As a result, there can be less size disparity between the foreground and backdrop.
– During mitotic identification, it aids in reducing categorization, end-effectors, and localization degradation.

The other sections of the research were structured so that section 2 explains the database, characteristics, and categorization of the IMFRCNN. While section 3 gives a review of the literature. Outcomes are covered in section 4. Lastly, conclusion and recommendations for further research are covered in section 5.

2. METHOD

The proposed approach modifies the IMFRCNN architecture, incorporating ResNet101 pre-trained weights from the common objects in context (COCO) 2017 dataset. In addressing the challenges posed by histopathology images, particularly with mitotic nuclei's poor visual ratio, and deep learning models undergo crucial preprocessing stages. Utilizing ResNet101 features such as pooling, convolutional layers with stride 2, and strategic max-pooling, the method aims to reduce image size, preserve rich information, and prevent the disappearance of small items. This enhances the feature extractor's ability to discern meaningful characteristics within histopathological images.

2.1. Dataset description

Researchers have used a breast cancer dataset in this study is a histopathological database. Figure 1 illustrates the 9,109 microscopic images of breast tumor tissue obtained from 82 patients utilizing various magnification variables that comprise the breast cancer histopathological imaging classification. It now has 2,480 benign samples and 5,429 cancerous ones. In addition to the PandD Laboratory for Pathological Anatomy and Cytopathology in Parana, this database was developed. Since it enables future comparison and assessment, humans think that researchers would consider this dataset to be beneficial [31]. Cancer was referred to as a malignant tumor since the lesion can spread to distant areas, invade other tissues, and lead to death.

Researchers investigate hidden trends in the information using advanced analytics. Three files were produced. The real bounding boxes for every class, in addition to the classes. Following the training phase, researchers make predictions using these images. The name of the image, the class, and the bounding box coordinates has all been stored in this folder. More than one object may be present in a single photograph. Hence, there could be more rows in a single image.

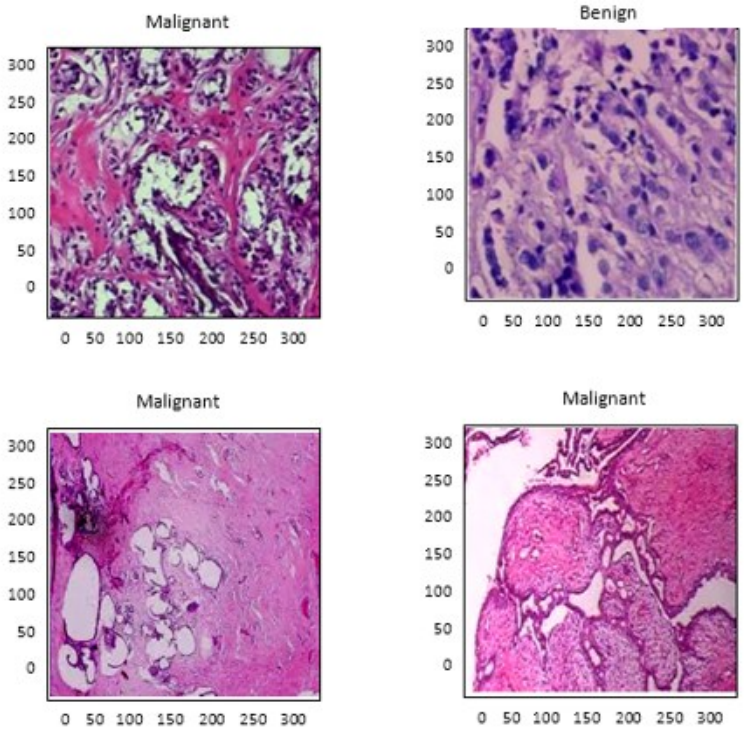

Figure 1. Histopathological image dataset for breast cancer

2.2. Methodology

The IMFRCNN architecture has been tweaked to create the proposed approach. The IMFRCNN with ResNet101 pre-trained weights from the COCO 2017 dataset were utilized in this system. One of the crucial stages of models based on deep learning was pre-processing. To improve the contrasts, a variety of preprocessing methods have been used, including random adjustments of comparison, brightness, and hue. Mitotic nuclei have a poor visual ratio in histopathology images. The image-to-object ratio was strong in these kinds of photos since the nuclei were tiny [20].

Pooling and a few convolutional layers with stride 2 were features of the ResNet101 that seem to be useful for reducing the length of both the input image and the objects included within it. As we previously explained, one goal of employing a pooling layer would be to decrease image size while maintaining rich information. After max-pooling, the stretched layers enlarge objects while maintaining the dimensions of the supplied images by using the rich information obtained from the output of max-pooling. Thus, after the max-pooling layer, a stretched layer was utilized to prevent the disappearance of items. This method lowers the likelihood of small items disappearing, as illustrated in Figure 2, which aids the feature extractor in learning the good characteristics of in-depth blocks. Although big-scale increments at once affect the shape of nuclei, a high dilated rate was advantageous for increasing object size [24].

The morphology of mitotic and non-mitotic nuclei with similar shapes and sizes was altered by more dilated layers. Using only 3 expanded levels out of ResNet101's total of 101 layers was intended to prevent small items from dissipating in deep layers while maintaining the shape of nuclei. IMFRCNN has been generated in conv3 block1, conv4 block1, and conv3 block2, as shown in Figure 3 dilated convolutional node.

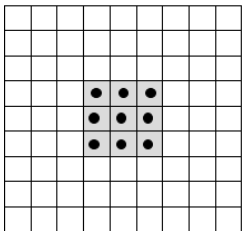

Figure 2. Filter without dilation rate

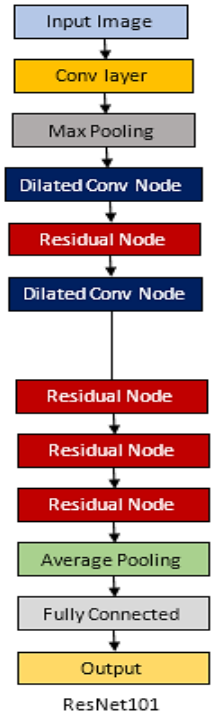

Figure 3. A dilated convolutional node

Regardless of the size of the input, the region of interest (ROI) pooling layer separates the proposed regions' characteristics into smaller areas and outputs fixed-size characteristics. The ROI pooling layer's result in the proposed method was 7×7. The next fully connected layers, SoftMax, including bounding box extrapolation branches, would then be given the result characteristics of the ROI pooling layers in IMFRCNN as illustrated in Figure 4.

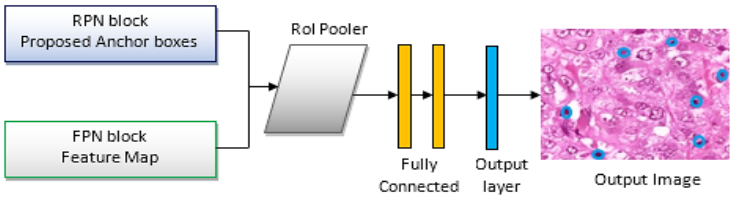

Figure 4. ROI block for localization and categorization on IMFRCNN

2.3. Improved faster recurrent convolutional neural network

To identify distinct items in an image and create a bounding box around a particular object, techniques called object recognition and segmentation have been used. One technique for object recognition and segmentation was a convolutional neural network-based multi-scale local and global feature representation (MFR-CNN) [32]. MFR-CNN serves as the foundation for mask R-CNN, which expands its use in picture categorization. Figure 5 shows how its network architecture was structured.

The procedure results in the loss of data sources, causing the ROI and extracted characteristics of the original image to be displaced. Following the completion of the network design, the MFR-CNN was learned using the ultrasound images, the matching biopsy information, and the radiologist-drawn tumor contours as the ground truth [22]. The information from the training set was utilized to build a model, which was subsequently evaluated against the validity collection to make sure it was accurate and stable. The training technique divided randomly the gathered instances into a training dataset and testing set. IMFRCNN's model function loss was described as in (1).

$$L = Lclass + Lbox + Lmask \tag{1}$$

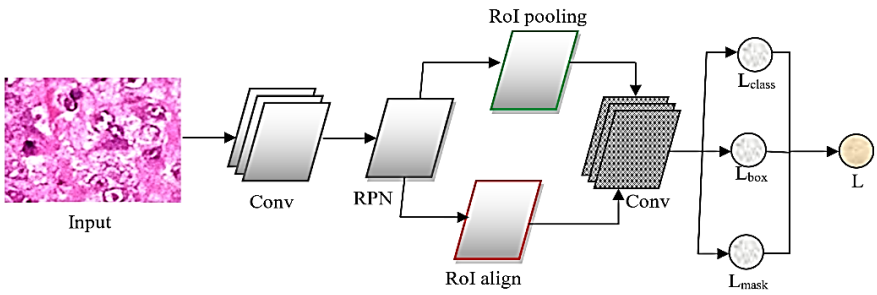

Figure 5. IMFRCNN's structure

Mean average precision (mAP) is to measure the lesion detection/segmentation efficiency on the testing set and trained MFR-CNN model as given in (2). Where A is segmentation of model results; B is the appropriate tumor outline expert radiologist has drawn as a real clinical lesion. N_x^{DR} seems to be the overlapping area between the model-identified lesion and also the genuine medical lesion regions have real clinical lesions size. N_t stands for the number of images. Reliability was utilized to confirm the proposed method's overall lesion categorization efficiency. In (3) analyze the evaluation measures such as true positive (TP), true negative (TN), false positive (FP), and false positive (FN).

$$mAP = \frac{A \cap B}{A \cup B} = \frac{1}{N_t} \sum_{x=1}^{N_t} \left(\frac{N_x^{DR}}{N_x^{D}} \right) \tag{2}$$

$$Accuracy = (TP + TN)/(TP + TN + FP + FN) \tag{3}$$

3. RESULTS AND DISCUSSION

The outcomes of the radiologists' tumor contour analysis have been displayed in Figure 6. Breast ultrasound images of two separate malignant tumors can be seen in Figure 6(a), while benign tumors can be seen in Figure 6(b). The actual reference image occupies the left side of the image, and also the real masking created by a qualified radiologist using the original image has been shown on the right side.

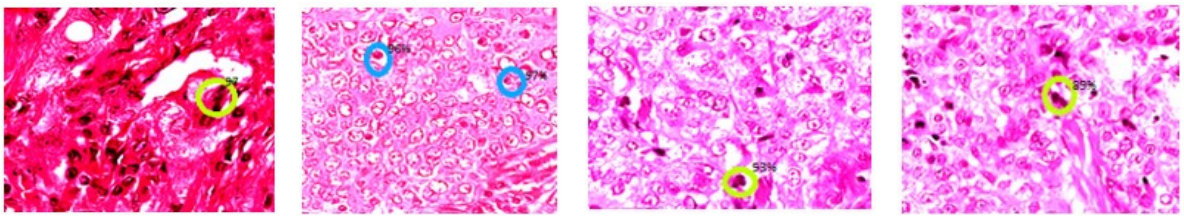

(a) (b)

Figure 6. Detections of samples (a) malignant tumor and (b) benign tumor

The learning algorithm continuously reduced until the conclusion of 25K iterations, after 2.3K iterations. By including a total of 100 bounding boxes for every category, the largest amount of anchor boxes in regional proposal network (RPN) was set to 300, whereas in the outcome, it must be set to 200. A variety of blocks in the proposed IMFRCNN employ varying numbers of dilated layers using variable rates of dilation. Applying dilated layers using dilation rates that vary between 2 to 5. All variations' outcomes can be seen in Figure 7.

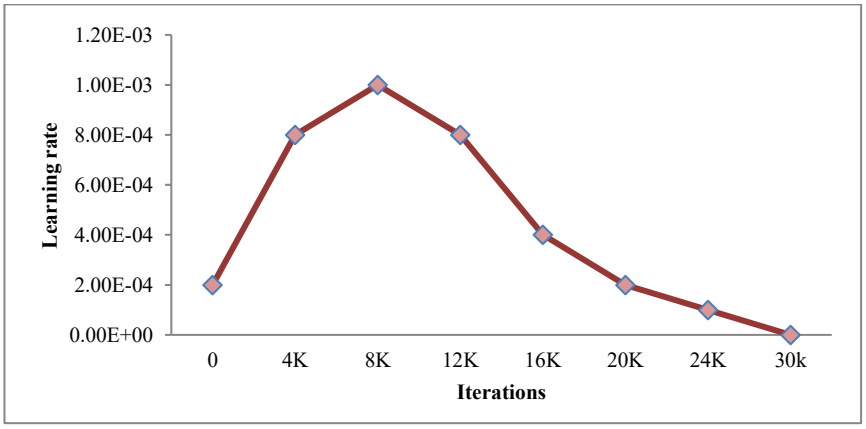

Figure 7. Rate of learning

Loss behavior in general indicates that the model progressively acquired better features for region suggestions. Ultimately, the proposed model's overall loss has been estimated and seems to be 0.15, as shown in Figure 8. The total loss was 0.52 after the first iteration and climbed to 0.7 after 7K iterations. The unpredictability of categorization, RPN objectless and localization loss up to 2.1K iterations seems to be the source of the overall loss's rising behavior. After 2.1K iterations, all losses dropped gradually, resulting in a reduction in the overall loss. It was found that the losses of the IMFRCNN dropped as the number of iterations increased, indicating that the proposed model learned more effectively as repeats were added. Typical object recognition algorithms have been honed for 25K steps in the same surroundings. All experimental models' outcomes were contrasted with those of the proposed IMFRCNN. The proposed model outperformed the opposition regarding average accuracy. According to Table 1, the proposed method performed better for the average precision (AP) and mAP accuracy measures.

The proposed model performs best for median memory when compared to existing conventional methods for identifying objects. The proposed framework performed the best at AP and mAP as shown in Table 2. When model allow identifying one object in a given image its mean recollection as AP.

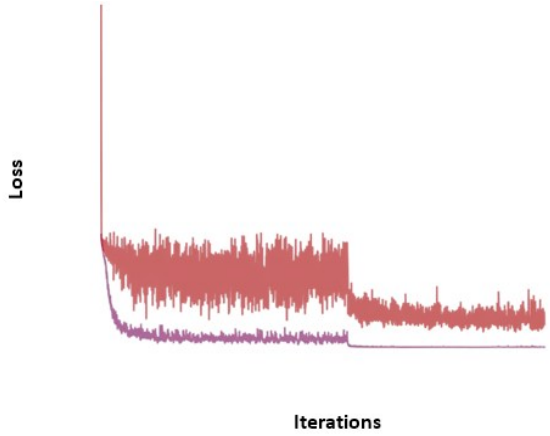

Figure 8. The proposed model's overall loss of average accuracy

Table 1. Comparison of the proposed and existing system accuracy

Techniques	Backbone	AP	mAP
16	ResNet101	19.78	21.89
18	EfficientNet	24	24.68
21	ResNet101	16.62	18.00
Proposed model	Modified ResNet101	25.38	26.18

Table 2. Comparison of the proposed models based on memory

Techniques	Backbone	AP	mAP
16	ResNet101	14.5	47.5
18	EfficientNet	15.6	37.8
21	ResNet101	12.3	41.5
Proposed model	Modified ResNet101	15.6	52.5

Outcomes from object detection models were presented as bounding boxes using class labels. Figure 9 displays the top 5 models' results. In predicted results, frames represent expected non-mitotic nuclei, while green bounding boxes represent projected mitotic nuclei. Due to the intricacy of the images, the object recognition performance of the model in histopathological images remains very low. The other causes of poor achievement were intra-class heterogeneity and inter-class homogeneity. The absence of tiny items, moreover, meant that the feature extractor's efficiency stayed poor. To prevent small items from vanishing, various numbers of dilated levels at different hierarchical levels with varied dilatation speeds were utilized. The best outcomes were finally obtained with 3 dilated layers with a dilatation frequency of 2. Three crucial parameters that aid the feature extractor seem to be the location of dilated layers and their rate of dilatation.

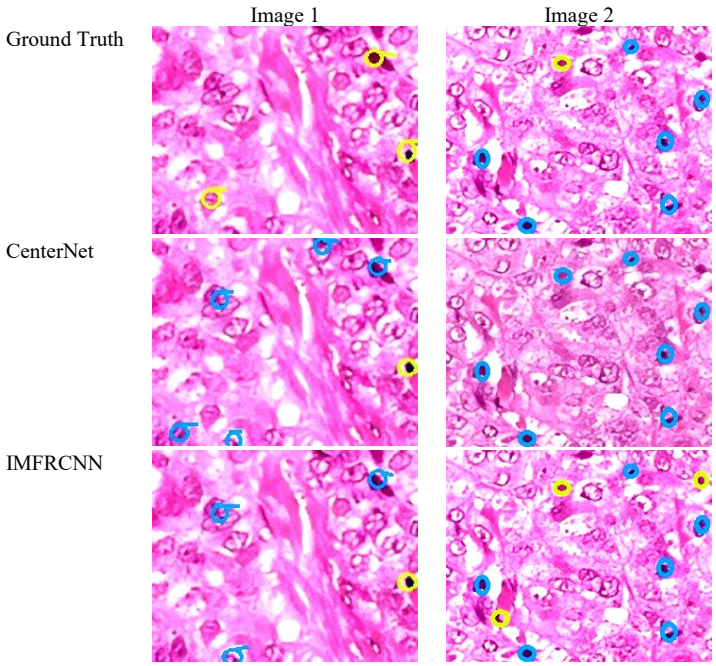

Figure 9. Comparison of various models using actual data

The most advanced model for identifying tiny objects, including such mitotic and non-mitotic nuclei seems to be the IMFRCNN. Utilizing domain adaptability and multi-model features fusion would help the IMFRCNN perform better. When a model learns from image features to microscopic images, its performance suffers. The structural differences between normal and microscopic images seem to be the cause of inferior performance. Using weights that have already been trained in the same domain might improve performance. In the process of transferring weights, the model must first be trained on microscopic images. The feature extractor determines how well a model performs. The architecture of histopathology images was complicated, stand-alone pattern extractors might well have trouble extracting characteristics. A different approach to extracting rich features might therefore be to be using numerous models for extracting features.

Implemented both a normal faster recurrent convolutional neural network (normal FRCNN) and a FRCNN alone to demonstrate the effectiveness of our unique two-stage top-down cascade multi-scale suggestion-generating technique. The effectiveness of our proposed model in comparison to the other two benchmark models can be seen in Table 2. The IMFRCNN algorithm was enhanced by our unique proposal network for regions. Our contribution raises the bar for computerized breast cancer prognosis, potentially moving it closer to clinical practice becoming entirely automated. Figure 10 shows the confusion matrix.

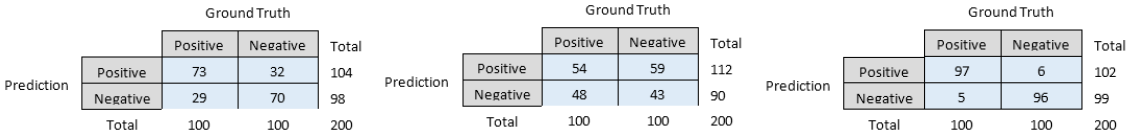

Figure 10. Confusion matrix

4. CONCLUSION

To quickly and accurately identify mitotic figures in breast cancer histopathology pictures, researchers suggest a novel IMFRCNN structure. In comparison to the earlier proposed research, our findings highlight the strength of our proposed model. The highest accuracy to date was achieved by our proposed model, which had an F-score value of 0.955. To identify mitotic figures, our model utilizes the characteristics that were learned, demonstrating the superiority of learning features over characteristics that were created. Further studies for mitotic detection and counting using whole-slide imaging (WSI) could be conducted. Similarly to this, a hybrid model might be added to the object segmentation model's foundation to extract better features and improve efficiency.

ACKNOWLEDGMENTS

We would like to express our heartfelt thanks to our guide for his unwavering guidance, invaluable insights, and encouragement throughout the research process.

FUNDING INFORMATION

No funding is raised for this research.

AUTHOR CONTRIBUTIONS STATEMENT

This journal uses the Contributor Roles Taxonomy (CRediT) to recognize individual author contributions, reduce authorship disputes, and facilitate collaboration.

Name of Author	C	M	So	Va	Fo	I	R	D	O	E	Vi	Su	P	Fu
Pattan M. D. Ali Khan	✓	✓	✓		✓	✓		✓	✓	✓	✓		✓	
Xavier Arputha Rathina	✓	✓		✓	✓	✓		✓	✓	✓	✓	✓		

C : **C**onceptualization
M : **M**ethodology
So : **So**ftware
Va : **Va**lidation
Fo : **Fo**rmal analysis
I : **I**nvestigation
R : **R**esources
D : **D**ata Curation
O : Writing - **O**riginal Draft
E : Writing - Review & **E**diting
Vi : **Vi**sualization
Su : **Su**pervision
P : **P**roject administration
Fu : **Fu**nding acquisition

CONFLICT OF INTEREST STATEMENT

Authors state no conflict of interest.

INFORMED CONSENT

We have obtained informed consent from all individuals included in this study.

ETHICAL APPROVAL

The research related to human use has been complied with all the relevant national regulations and institutional policies in accordance with the tenets of the Helsinki Declaration and has been approved by the authors' institutional review board or equivalent committee.

DATA AVAILABILITY

The data that support the findings of this study are openly available in Computers & Electrical Engineering at http://doi.org/10.1016/j.compeleceng.2021.107038, reference number [31].

REFERENCES

[1] L. Alzubaidi *et al.*, "Review of deep learning: concepts, CNN architectures, challenges, applications, future directions," *Journal of Big Data*, vol. 8, no. 1, 2021, doi: 10.1186/s40537-021-00444-8.

[2] T. Mahmood, M. Arsalan, M. Owais, M. B. Lee, and K. R. Park, "Artificial intelligence-based mitosis detection in breast cancer histopathology images using faster R-CNN and deep CNNs," *Journal of Clinical Medicine*, vol. 9, no. 3, 2020, doi: 10.3390/jcm9030749.

[3] S. Y. Siddiqui *et al.*, "IoMT cloud-based intelligent prediction of breast cancer stages empowered with deep learning," *IEEE Access*, vol. 9, pp. 146478–146491, 2021, doi: 10.1109/ACCESS.2021.3123472.

[4] J. V. D. Laak, G. Litjens, and F. Ciompi, "Deep learning in histopathology: the path to the clinic," *Nature Medicine*, vol. 27, no. 5, pp. 775–784, 2021, doi: 10.1038/s41591-021-01343-4.

[5] P. Harrison and K. Park, "Tumor detection in breast histopathological images using faster R-CNN," in *2021 International Symposium on Medical Robotics*, 2021, pp. 1–7, doi: 10.1109/ISMR48346.2021.9661483.

[6] A. D. Pratiwi and I. P. Sari, "Robust breast cancer detection using faster R-CNN algoritma," *International Journal of Informatics and Computation*, vol. 4, no. 1, 2022, doi: 10.35842/ijicom.v4i1.49.

[7] K. G. Chaudhari, "Comparative analysis of CNN models to diagnose breast cancer," *International Journal of Innovative Research in Science, Engineering and Technology*, vol. 7, no. 10, pp. 8180–8187, 2018, doi: 10.15680/IJIRSET.2018.0710074.

[8] H. Huang, X. Feng, J. Jiang, P. Chen, and S. Zhou, "Mask RCNN algorithm for nuclei detection on breast cancer histopathological images," *International Journal of Imaging Systems and Technology*, vol. 32, no. 1, pp. 209–217, 2022, doi: 10.1002/ima.22618.

[9] L. Liu *et al.*, "Collaborative transfer network for multi-classification of breast cancer histopathological images," *IEEE Journal of Biomedical and Health Informatics*, vol. 28, no. 1, pp. 110–121, 2024, doi: 10.1109/JBHI.2023.3283042.

[10] S. Ayashm, M. Valizadeh, M. C. Amirani, and S. Mihandoost, "Mitosis detection in breast histopathology images using a self-attention-enhanced Faster R-CNN framework," *IEEE Access*, vol. 14, pp. 16455–16469, 2026, doi: 10.1109/ACCESS.2026.3658646.

[11] V. Patel, V. Chaurasia, R. Mahadeva, and S. P. Patole, "GARL-Net: graph based adaptive regularized learning deep network for breast cancer classification," *IEEE Access*, vol. 11, pp. 9095–9112, 2023, doi: 10.1109/ACCESS.2023.3239671.

[12] Y. Kawazoe *et al.*, "Faster R-CNN-based glomerular detection in multi-stained human whole slide images," *Journal of Imaging*, vol. 4, no. 7, 2018, doi: 10.3390/jimaging4070091.

[13] S. A. Sánchez, A. D. Morales, M. F. Arroyo, and y. H. D. Asís, "Artificial intelligence model for the prediction of malignant tumors using a set of medical images from mammography studies," *IOP Conference Series: Materials Science and Engineering*, vol. 1154, no. 1, 2021, doi: 10.1088/1757-899X/1154/1/012013.

[14] N. Dif and Z. Elberrichi, "Deep learning methods for mitosis detection in breast cancer histopathological images: a comprehensive review," in *Artificial Intelligence and Machine Learning for Digital Pathology*, Cham, Switzerland: Springer, 2020, pp. 279–306, doi: 10.1007/978-3-030-50402-1_17.

[15] I. Sirazitdinov, M. Kholiavchenko, T. Mustafaev, Y. Yixuan, R. Kuleev, and B. Ibragimov, "Deep neural network ensemble for pneumonia localization from a large-scale chest X-ray database," *Computers & Electrical Engineering*, vol. 78, pp. 388–399, 2019, doi: 10.1016/j.compeleceng.2019.08.004.

[16] I. Girolami *et al.*, "Artificial intelligence applications for pre-implantation kidney biopsy pathology practice: a systematic review," *Journal of Nephrology*, vol. 35, no. 7, pp. 1801–1808, 2022, doi: 10.1007/s40620-022-01327-8.

[17] E. Uchino *et al.*, "Classification of glomerular pathological findings using deep learning and nephrologist–AI collective intelligence approach," *International Journal of Medical Informatics*, vol. 141, 2020, doi: 10.1016/j.ijmedinf.2020.104231.

[18] N. Altini *et al.*, "Semantic segmentation framework for glomeruli detection and classification in kidney histological sections," *Electronics*, vol. 9, no. 3, 2020, doi: 10.3390/electronics9030503.

[19] E. H. Nguyen *et al.*, "Circle representation for medical object detection," *IEEE Transactions on Medical Imaging*, vol. 41, no. 3, pp. 746–754, 2022, doi: 10.1109/TMI.2021.3122835.

[20] M. Aljabri, M. AlAmir, M. AlGhamdi, M. A. -Mottaleb, and F. C. -Mesa, "Towards a better understanding of annotation tools for medical imaging: a survey," *Multimedia Tools and Applications*, vol. 81, no. 18, pp. 25877–25911, 2022, doi: 10.1007/s11042-022-12100-1.

[21] R. G. -Caballero, C. J. G. -Orellana, A. G. -Manso, H. M. G. -Velasco, R. T. -Molina, and M. M. -Macías, "Precise pollen grain detection in bright field microscopy using deep learning techniques," *Sensors*, vol. 19, no. 16, 2019, doi: 10.3390/s19163583.

[22] Y. Lu *et al.*, "Identification of metastatic lymph nodes in MR imaging with faster region-based convolutional neural networks," *Cancer Research*, vol. 78, no. 17, pp. 5135–5143, 2018, doi: 10.1158/0008-5472.CAN-18-0494.

[23] H. Soltani, M. Amroune, I. Bendib, and M. Y. Haouam, "Breast cancer lesion detection and segmentation based on mask R-CNN," in *2021 International Conference on Recent Advances in Mathematics and Informatics (ICRAMI)*, 2021, pp. 1–6, doi: 10.1109/ICRAMI52622.2021.9585913.
[24] T. P. Latchoumi, G. Kalusuraman, J. F. Banu, T. L. Yookesh, T. P. Ezhilarasi, and K. Balamurugan, "Enhancement in manufacturing systems using grey-fuzzy and LK-SVM approach," in *2021 IEEE International Conference on Intelligent Systems, Smart and Green Technologies (ICISSGT)*, 2021, pp. 72–78, doi: 10.1109/ICISSGT52025.2021.00026.
[25] A. Sohail, A. Khan, N. Wahab, A. Zameer, and S. Khan, "A multi-phase deep CNN based mitosis detection framework for breast cancer histopathological images," *Scientific Reports*, vol. 11, no. 1, 2021, doi: 10.1038/s41598-021-85652-1.
[26] B. Sheng, M. Zhou, M. Hu, Q. Li, L. Sun, and Y. Wen, "A blood cell dataset for lymphoma classification using faster R-CNN," *Biotechnology & Biotechnological Equipment*, vol. 34, no. 1, pp. 413–420, 2020, doi: 10.1080/13102818.2020.1765871.
[27] B. Gami, K. Chauhan, and B. Y. Panchal, "Breast cancer detection using deep learning," in *Mobile Radio Communications and 5G Networks*, 2023, pp. 85–95, doi: 10.1007/978-981-19-7982-8_8.
[28] X. Li, Z. Xu, X. Shen, Y. Zhou, B. Xiao, and T.-Q. Li, "Detection of cervical cancer cells in whole slide images using deformable and global context aware faster RCNN-FPN," *Current Oncology*, vol. 28, no. 5, pp. 3585–3601, 2021, doi: 10.3390/curroncol28050307.
[29] S. Jarujunawong and P. Horkaew, "Enhancing AI-Driven diagnosis of invasive ductal carcinoma with morphologically guided and interpretable deep learning," *Applied Sciences*, vol. 15, no. 12, 2025, doi: 10.3390/app15126883.
[30] B. Murugesan, S. Selvaraj, K. Sarveswaran, K. Ram, J. Joseph, and M. Sivaprakasam, "Deep detection and classification of mitotic figures," in *Medical Imaging 2019: Digital Pathology*, 2019, doi: 10.1117/12.2508770.
[31] X. Pan *et al.*, "Mitosis detection techniques in HandE stained breast cancer pathological images: a comprehensive review," *Computers & Electrical Engineering*, vol. 91, 2021, doi: 10.1016/j.compeleceng.2021.107038.
[32] Y. Zhao, J. Zhang, D. Hu, H. Qu, Y. Tian, and X. Cui, "Application of deep learning in histopathology images of breast cancer: a review," *Micromachines*, vol. 13, no. 12, 2022, doi: 10.3390/mi13122197.

BIOGRAPHIES OF AUTHORS

Pattan M. D. Ali Khan earned his Bachelor's of Technology B.Tech. degree in Computer Science Engineering from JNTUA in 2005. He has obtained his Master's degree in M.E. (Computer Science Engineering) from St. Peter's University in 2012. Currently, he is a research scholar at B. S. Abdur Rahman Crescent Institute of Science and Technology (Deemed to be University) doing his Ph.D. in Computer Science and Engineering. He has attended many workshops and induction programs conducted by various Universities. His areas of interest are machine learning and image processing. He can be contacted at email: alik_12@rediffmail.com.

Xavier Arputha Rathina is an associate professor in Department of Computer Science and Engineering at School of SCIMS of B. S. Abdur Rahman Crescent Institute of Science and Technology (Deemed to be University) Chennai with an experience of 27 years in teaching. She did her B.E. in Electronics Communication Engineering and Master's degree in Computer Science and Engineering, and Ph.D. in Computer Science and Engineering. Her areas of interest are image processing, emotional intelligence, and speech processing. She can be contacted at this email: xarathina@crescent.education.